ELSEVIER

Astrophysical constraints from gamma-ray spectroscopy

Roland Diehl [a,*], Nikos Prantzos [b], Peter von Ballmoos [c]

[a] *Max-Planck-Institut für extraterrestrische Physik, D-85741 Garching, Germany*
[b] *Institut d'Astrophysique, F-75014 Paris, France*
[c] *Centre d'Étude Spatiale des Rayonnements, F-31028 Toulouse, France*

Abstract

Gamma-ray lines from cosmic sources provide unique isotopic information, since they originate from energy level transitions in the atomic nucleus. Gamma-ray telescopes explored this astronomical window in the past three decades, detecting radioactive isotopes that have been ejected in interstellar space by cosmic nucleosynthesis events and nuclei that have been excited through collisions with energetic particles. Astronomical gamma-ray telescopes feature standard detectors of nuclear physics, but have to be surrounded by effective shields against local instrumental background, and need special detector and/or mask arrangements to collect imaging information. Due to exceptionally-low signal/noise ratios, progress in the field has been slow compared with other wavelengths. Despite the difficulties, this young field of astronomy is well established now, in particular due to advances made by the Compton Gamma-Ray Observatory in the 90ies. The most important achievements so far concern: short-lived radioactivities that have been detected in a couple of supernovae (^{56}Co and ^{57}Co in SN1987A, ^{44}Ti in Cas A), the diffuse glow of long-lived ^{26}Al that has been mapped along the entire plane of the Galaxy, several excited nuclei that have been detected in solar flares, and, last but not least, positron annihilation that has been observed in the inner Galaxy since the 70ies. High-resolution spectroscopy is now being performed: since 2002, ESAs INTEGRAL and NASAs RHESSI, two space-based gamma-ray telescopes with Ge detectors, are in operation. Recent results include: imaging and line shape measurements of e^-–e^+ annihilation emission from the Galactic bulge, which can hardly be accounted for by conventional sources of positrons; ^{26}Al

* Corresponding author.
  E-mail address: rod@mpe.mpg.de (R. Diehl).

emission and line width measurement from the inner Galaxy and from the Cygnus region, which can constrain the properties of the interstellar medium; and a diffuse ^{60}Fe gamma-ray line emission which appears rather weak, in view of current theoretical predictions. Recent Galactic core-collapse supernovae are studied through ^{44}Ti radioactivity, but, apart from Cas A, no other source has been found; this is a rather surprising result, assuming a canonical Galactic supernova rate of $\sim 1/50$ years. The characteristic signature of ^{22}Na-line emission from a nearby O–Ne–Mg novae is expected to be measured during INTEGRALs lifetime.

1. Overview

Radioactive isotopes are common by-products of nucleosynthesis in cosmic sources and constitute important probes of the underlying physical processes, as they can be studied through their characteristic gamma-ray emission. Candidate sources are supernovae and novae, but also the winds from massive stars and intermediate stars on the asymptotic giant branch (AGB stars). Similarly, collisions of nuclei that have been accelerated to cosmic-ray energies produce de-excitation gamma-rays, which can be used to study the physics of the acceleration sites, as in the case of solar flares.

Radioactive nuclei are thermonuclearly synthesized in the hot and dense stellar interiors, which are opaque to γ-rays. Released γ-ray photons interact with the surrounding material and are Compton-scattered down to X-ray energies, until they are photoelectrically absorbed and their energy is emitted at longer wavelengths. To become detectable, radioactive nuclei have to be brought to the stellar surface (through vigorous convection) and/or ejected in the interstellar medium, either through stellar winds (asymptotic giant branch and Wolf–Rayet stars) or through an explosion (novae or supernovae). Their direct detection provides then unique information on their production sites, which cannot be obtained through observations at other wavelengths. Thus it complements other methods used for the study of cosmic nucleosynthesis, which are often indirect or plagued with instrumental difficulties. Those methods exploit X-ray/low-energy gamma-ray continuum emission arising from the effect of comptonization, characteristic X-ray recombination lines from highly-ionized species, and laboratory isotopic analysis of presolar grains included in meteorites [158].

Obviously, radionuclides of interest for γ-ray line astronomy are those with high enough yields and short enough lifetimes for the emerging γ-ray lines to be detectable. On the basis of those criteria, Table 1 gives the most important radionuclides (or radioactive chains) for γ-ray line astronomy, along with the corresponding lifetimes, line energies and branching ratios, production sites and nucleosynthetic processes.

When the lifetime of a radioactive nucleus is not very large w.r.t. the timescale between two nucleosynthetic events in the Galaxy, those events are expected to be seen as *point-sources* in the light of that radioactivity. In the opposite case a *diffuse emission* in the Galaxy is expected from the cumulated emission of hundreds or thousands of sources. Characteristic timescales between two explosions are $\sim$1–2 weeks for novae (from their estimated Galactic frequency of $\sim$25–30 yr^{-1} [1], $\sim$50–100 yr for supernova types II + Ib, and $\sim$200–400 yr for SNIa (from the corresponding Galactic frequencies

Table 1
Important stellar radioactivities for gamma-ray line astronomy

Decay chain	Mean life* (yr)	Line energies (MeV) (Branching ratios)	Site [Detected]	Nuclear process
$^7Be \to {}^7Li$	0.21	0.478 (0.1)	Novae	Expl.H
$^{56}Ni \to {}^{56}Co^+ \to {}^{56}Fe$	0.31	<u>0.847</u> (1.0) <u>1.238</u> (0.68) 2.598 (0.17) 1.771 (0.15)	SN [SN1987A] [SN1991T]	NSE
$^{57}Co \to {}^{57}Fe$	1.1	<u>0.122</u> (0.86) <u>0.136</u> (0.11)	SN [SN1987A]	NSE
$^{22}Na^+ \to {}^{22}Ne$	3.8	1.275 (1.0)	Novae	Expl.H
$^{44}Ti \to {}^{44}Sc^+ \to {}^{44}Ca$	89	<u>1.157</u> (1.0) <u>0.068</u> (0.95) <u>0.078</u> (0.96)	SN [Cas A]	α-NSE
$^{26}Al^+ \to {}^{26}Mg$	1.04×10^6	<u>1.809</u> (1.0)	WR, AGB Novae SNII [inner Galaxy,Vela, Cygnus, Orion]	St.H Expl.H St.Ne Expl.Ne ν
$^{60}Fe \to {}^{60}Co \to {}^{60}Ni$	2.2×10^6	<u>1.332</u> (1.0) <u>1.173</u> (1.0)	SN [Galaxy]	n-capt
e^+	10^5–10^7	<u>0.511</u>	SNIa... [Galactic bulge]	β^+-decay

+: positron emitters (associated 511 keV line); ∗: double decay chains: the longest lifetime is given; Underlined: lines detected; In parentheses: branching ratios; In brackets: sites of lines detected; St.(Expl): hydrostatic (explosive) burning; NSE: nuclear statistical equilibrium; α: α-rich "freeze-out"; n-capt: neutron captures; ν: neutrino-process.

of $\sim$3 SNII + SNIb century^{-1} and $\sim$0.25–0.5 SNIa century^{-1}, [2]). Comparing those timescales to the decay lifetimes of Table 1, one sees that in the case of long-lived ^{26}Al and ^{60}Fe *diffuse* emission is expected; the spatial profile of such emission should reflect the Galactic distribution of the underlying sources, if the ejected nuclei do not travel too far away from their sources during their radioactive lifetime. All the other radioactivities of Table 1 should be seen as *point sources* in the Galaxy, except, perhaps, ^{22}Na from Galactic novae in the central bulge. Indeed, the most prolific ^{22}Na producers, O–Ne–Mg rich novae, have a frequency $\sim$ 1/3 of the total (i.e., $\sim$10 yr^{-1}), resulting in $\sim$40 active sources in the Galaxy during the 3.8 yr lifetime of ^{22}Na.

In principle, the intensity of the escaping γ-ray lines gives important information on the yields of the corresponding isotopes, on the physical conditions (temperature, density, neutron excess, etc.) in the stellar zones of their production, and on other features of the production sites (extent of convection, mass loss, hydrodynamic instabilities, position of the "mass-cut" in core-collapse SN, etc.). Moreover, the shape of the γ-ray lines reflects the velocity distribution of the ejecta, modified by the opacity along the line of sight and can give information on the structure of the ejecta, and on the interstellar medium surrounding sources of nucleosynthesis.

At this point, the main advantages of the study of nucleosynthesis through the detection of the characteristic γ-ray lines of radioactivities should be clear:

- The unique possibility to *unambiguously identify isotopes*, which are the direct products of nuclear reactions. Indeed, elementary abundances (usually revealed by observations in most other wavelengths) may give ambiguous messages, since they may be the sum of different isotopes, produced by different processes in different physical conditions. Isotopic measurements from presolar grains may be affected by various physico-chemical effects, therefore astrophysical interpretations depend on models for such processes. In contrast, radioactive decay in interstellar space is mostly unaffected by physical conditions in/around the source such as temperature or density (except for the case of electron-capture radioactivities, see Section 3.1 for the case of ^{44}Ti).
- Decay gamma-rays are not attenuated along the line-of-sight due to their *highly penetrating nature* (attenuation length $\simeq$ few g cm^{-2}), thus probing stellar regions which are not accessible at other wavelengths.

The measurement of such decay gamma-rays with satellite-borne telescopes occurs in near-earth space, above the Earth's atmosphere (which is optically thick to gamma-rays, and is by itself a bright gamma-ray source from cosmic-ray interactions). The technique of gamma-ray telescopes is complex [3], and still in specific aspects less precise than alternative isotopic abundance measurements. With present-day spatial resolutions of the order of a degree it cannot compete with current X-ray telescopes such as Chandra and XMM-Newton to, e.g., map the ^{44}Ti distribution within the Cas A supernova remnant. Furthermore, local background from activation of the spacecraft and instrument through their irradiation with cosmic ray particles is high, leading to signal-to-background ratios which are of the order of 1/100; this is orders of magnitude worse than in laboratory measurements on presolar grain abundances, and effectively limits the sensitivity to γ-ray fluxes of a few 10^{-6} photons cm^{-2} s^{-1} for realistic observing times. Therefore, present-day instruments can access only sources in our Galaxy (and up to 10 Mpc in the case of strong ^{56}Co lines from SNIa), which are sufficiently bright for γ-ray line measurements. On the other hand, fields of view are of the order of sr, very much larger than in X-ray and even more in optical/IR telescopes; this allows for all-sky mapping and monitoring to an extent which is often impossible in these other fields of astronomy.

In the past three decades, various gamma-ray telescopes have established the following major features in the field of gamma-ray line astronomy [4,5]:

- Interstellar ^{26}Al has been mapped along the plane of the Galaxy, confirming that nucleosynthesis is an ongoing process in the Milky Way [6–8]; quite recently, the detection of ^{60}Fe has also been reported, bringing complementary (and poorly understood yet) information.
- Characteristic Co decay gamma-ray lines have been observed from SN1987A [9–11], directly confirming core-collapse supernova production of fresh isotopes belonging to the iron group. A marginally significant signal from Co decay has been reported in the case of the thermonuclear supernova SN1991T [12].
- ^{44}Ti gamma-rays have been discovered [13,14] from the young supernova remnant Cas A, confirming models of explosive nucleosynthesis in core-collapse supernovae.

- A diffuse glow of positron annihilation gamma-rays has been recognized from the direction of the inner Galaxy [15,16]; its intensity appears to be only marginally consistent with nucleosynthetic production of β^+-decaying radioactive isotopes.

In the following, we discuss those issues in some detail, after a brief introduction to the relevant theoretical background in the next section.

2. Production sites for gamma-ray emitting isotopes

Most of the radioactivities in Table 1 are synthesised in supernovae, either in core-collapse (ccSNe) or in thermonuclear (SNIa) explosions. This is the case, in particular, for the isotopes of the Fe-peak, ^{44}Ti, ^{56}Ni and ^{57}Co, which are produced by explosive Si-burning in the innermost stellar layers. Long-lived ^{60}Fe and ^{26}Al are produced in massive stars both hydrostatically and explosively. In fact, ^{26}Al may also be produced in AGB stars and novae, but its distribution in the Milky Way (as mapped by the COMPTEL instrument aboard CGRO) suggests that those sources are minor contributors galaxywide (see Section 3.3). Finally, novae are expected to produce astrophysically interesting amounts of several radioactive light-element isotopes, in particular, ^{7}Be and ^{22}Na.

^{26}Al is produced by proton captures on ^{25}Mg, hence in stellar zones where either of the two reactants is abundant. This may happen either in the H-layers (H-burning core or shell) where protons are abundant, or in the Ne–O layers, where ^{25}Mg nuclei are abundant from Ne-burning reactions (Fig. 1). ^{26}Al produced in the H-core decays with its 1 Myr-lifetime, and is ejected only by the final explosion, unless strong mass loss uncovers the former H-core (Wolf–Rayet star), in which case it is also ejected through the stellar wind; this happens in non-rotating stars with initial masses above $\sim 30\ M_\odot$ at solar metallicity. In general, the more massive the star, the larger the fraction of hydrostatically produced ^{26}Al in interstellar space.
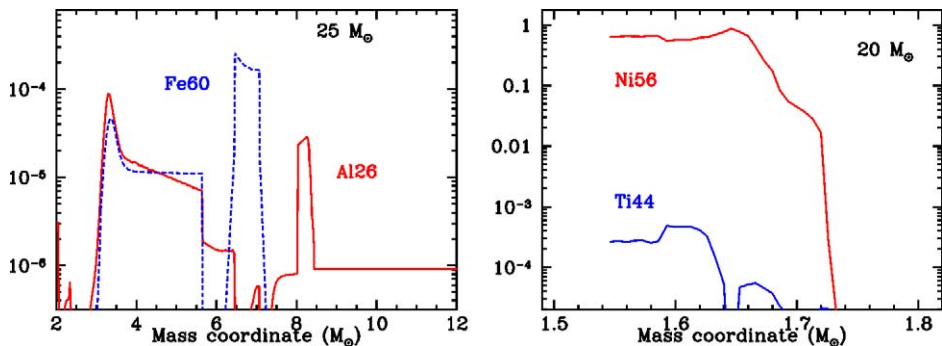

Fig. 1. Radial profiles of major radioactivities in core collapse supernovae [17]. Left: abundance profiles (mass fractions) of ^{26}Al (solid curve) and ^{60}Fe (dashed curve) inside an exploded 25 $M_\odot$ star; they are produced both hydrostatically (in the H- and He-layers, for ^{26}Al and ^{60}Fe, respectively) and explosively (both nuclei in the Ne–O layers). Right: profiles of ^{56}Ni and ^{44}Ti inside an exploded 20 $M_\odot$ star; the uncertain position of the "mass-cut" (around 1.5 $M_\odot$) makes difficult an accurate prediction of their yields.

The amount of ejected ^{26}Al depends on several factors: the specific criterion adopted for modelling convection (i.e., "Schwarzschild" vs. "Ledoux") determines the size of the convective stellar core and of the various burning shells. The reaction rate of ^{25}Mg$(p, \gamma)^{26}$Al is uncertain by a factor of ~ 2 in the relevant energy range (see, e.g., the regularly updated NACRE reaction rate compilation).[1] The still poorly known rate of the ^{12}C(α, γ) reaction determines the amount of ^{12}C left in the core at He-exhaustion and, therefore, the amount of ^{20}Ne produced through C-burning which, ultimately, determines the amount of ^{25}Mg (a product of Ne-burning) available for ^{26}Al production. Rotation has recently been introduced in massive star models. It induces diffusion of species from the core to the envelope and reduces the minimum initial mass for a star to become WR [18]. Finally, the abundant neutrinos from the collapsed stellar core may produce additional ^{26}Al by spallating ^{26}Mg nuclei in the Ne–O layers, the exact yield depending on the poorly known average neutrino energy [19].

For various reasons, there has been no self-consistent model of massive star evolution including all the ingredients concerning ^{26}Al production [147]. Models evolved up to the SN explosion did not include mass loss [19–21] and thus underestimated the hydrostatically produced part of ^{26}Al (because that amount of ^{26}Al decays inside the star while waiting for the explosion, whereas it is rapidly brought to the surface and ejected in the case of models with mass loss). On the other hand, models including mass loss (and other ingredients, like rotation) until recently did not follow the evolution until the final explosion and thus completely miss the explosive part of the yield of ^{26}Al. Finally, only the Santa–Cruz group of theoreticians [17,19] has included neutrino-induced nucleosynthesis in its model studies.

For all those reasons and uncertainties, it has been rather difficult up to now either to compare the yields of various groups or to make a self-consistent evaluation of the total amount of ^{26}Al expected to be ejected from a population of massive stars, covering the full mass range of 10 up to 100 $M_\odot$. Much attention has been paid to the comparison of hydrostatically-produced ^{26}Al as expelled through the winds of the most massive stars (WR), and the one produced (both hydrostatically and explosively) by somewhat less massive stars (below 30 $M_\odot$), for which mass loss is unimportant. Although such a comparison may appear futile, since it introduces an artificial separation between various stellar mass ranges, it played a pivotal role in the development of the whole field of the nucleosynthesis studies of ^{26}Al: indeed, it pushed theoreticians to continuous refinement of their models and a much more thorough exploration of the various factors and uncertainties affecting the ^{26}Al yields.

The case of ^{60}Fe, another long-lived isotope, again exemplifies such an approach to modeling of nucleosynthesis. ^{60}Fe is produced in the same zones as ^{26}Al (Ne–O zone), both hydrostatically and explosively, by successive n-captures on ^{58}Fe and ^{59}Fe. It is also produced in the base of the He-shell, by some mild r-process during the explosion [19] (see Fig. 1). Uncertainties on its yield are thus related to the cross section of n-capture on unstable ^{59}Fe and, of course, on the convection criterion employed. Contrary to the case of ^{26}Al, ^{60}Fe is expected to be ejected only by the SN explosion and not by the stellar wind,

---

[1] Web site at: http://pntpm.ulb.ac.be/nacre.htm.

since it is buried so deeply (in the Ne–O shell). For this reason, it has been suggested that detection of ^{60}Fe in the Galaxy would help to decide whether WR stars or core-collapse SN are the major sources of observed ^{26}Al (see Section 3.3).

This unfortunate artificial division between massive stars evolving with ∼constant mass and stars with mass loss is reaching an end now, since the first results of complete models (now including mass loss, but still no rotation, and reaching out to the SN stage) have been recently reported [22]; in those models, explosive ejection of ^{26}Al always appears to dominate the stellar-wind ejected ^{26}Al, even for the most massive stars (so much, in fact, that overproduction of ^{26}Al might become an issue...).

The other major radioactivities from massive stars (^{44}Ti, ^{56}Ni, ^{57}Co) are produced very near to the collapsed Fe-core of the star, by explosive Si-burning at temperatures $T > 4 \times 10^9$ K, or in the regime of nuclear statistical equilibrium (NSE, $T > 5 \times 10^9$ K). The production of ^{44}Ti also requires conditions of relatively low density, so that the alpha-particles which are abundantly produced during NSE do not quickly combine to form ^{12}C through the 3α reaction (which is very sensitive to density, being a 3-body reaction); a large fraction of mass in free α-particles after termination of NSE (the so-called α-*rich freeze-out*) is the necessary condition for significant production of ^{44}Ti. ^{56}Ni is mostly produced in the NSE phase, hence not sensitive to α-rich freeze-out, while ^{57}Co is mildly so. All three isotopes are produced in regions of small neutron excess (electron mole fractions $Y_e > 0.498$) and are very sensitive to the, still very poorly known, explosion mechanism (e.g., [23]); in particular, they are sensitive to the position of the "mass-cut", the fiducial surface separating the supernova ejecta from the material that falls back to the compact object after the passage of the reverse shock (see Fig. 1).

In the case of SN1987A, a supernova which occurred in the nearby Large Magellanic Cloud from a progenitor star with mass ∼ 18–20 $M_\odot$, the extrapolation of the optical light curve (powered by ^{56}Co radioactivity) to the origin of the explosion indicates a production of 0.07 $M_\odot$ of ^{56}Ni [24]; this is sometimes taken as a "canonical" yield of ^{56}Ni from ccSNe and often used in calculations of galactic chemical evolution. However, optical observations (albeit with large uncertainties) show that ccSNe display a wide range of ^{56}Ni values, correlated with the energy of the explosion [25]. The late lightcurve of SN1987A also constrains the amounts of other radioactivities and, in particular that of ^{44}Ti (see Section 3.1); however, only direct observations of the characteristic gamma-ray lines can confirm theoretical predictions. Care must be taken to acknowledge the diversity of events—ccSNe are not a homogeneous class of events.

NSE conditions are also encountered in the innermost regions of thermonuclearly exploding supernovae of type Ia. Uncertainties here are related to the progenitor system, to the way it reaches the Chandrasekhar mass and how it collapses, to the ignition density, and to the propagation of the nuclear flame (which determine the amount of electron captures and the degree of neutronisation of the ejecta, e.g., [26]). In thermonuclear supernova explosions, the evolution of flame speed determines the nucleosynthesis and in particular the total amount of ^{56}Ni produced. Anyone of the common SNe Ia scenarios (sub-Chandrasekhar, deflagration, delayed detonations, and pulsating delayed detonation models) seems able to produce a wide variety of ^{56}Ni masses, ranging from $\simeq 0.1$ to $1~M_\odot$ [27–29]. Generically, SNIa release about ten times as much ^{56}Ni than ccSNe. SNIa have lower envelope masses and higher expansion velocities than ccSNe (∼ 0.5 $M_\odot$ against

several $M_\odot$, and $\sim 2 \times 10^4$ km s^{-1} against $\sim 5 \times 10^3$ km s^{-1}), reflecting their presumed origin from a star which has previously lost its envelope. For those reasons they are expected to become transparent to γ-rays much earlier and to be much brighter γ-ray sources than ccSNe. The expected γ-ray line fluxes from the ^{56}Co decay, combined to sensitivities of present-day γ-ray instruments, limit observations of SNIa to rare events within about 15 Mpc (i.e., one every few years). Because of the lacking envelope, SNIa are expected to also be much more important sources of positrons than SNII (and, in fact, than any other known source), although the exact amount of escaping e$^+$ depends on poorly understood factors, like the intensity and configuration of the magnetic field in the exploded star (see Section 3.4).

In the light of the frequencies of occurrence of ccSNe and SNIa in external galaxies [2] it is a sign of fortune that SN1987A is the first, and, up to now, only one supernova which is clearly detected in the light of its radioactivity γ-rays. We still lack a complete picture on how radioactive energy is deposited inside supernovae into other forms of energy (radiating, or kinetic). In spite of the important γ-ray signals from SN1987A and Cas A, those are just two observed events, which may not sample an average ccSN, especially since core collapse by itself seems not so tightly regulated to produce a rather homogeneous event class such as SNIa are. Nevertheless, the physics of such radioactive-energy deposits probably will be revealed through observations of many more such events, probably then most directly in more signatures at γ-ray energies.

3. Specific isotopes and sources

3.1. Fe group nuclei and ^{44}Ti from supernovae

Thermonuclear supernovae   SN1991T occurred at a distance of 13 Mpc, and was a peculiar and exceptionally-bright supernova of the Ia type. Its Co decay lines were marginally detected (at a significance level of 3–5σ) with the COMPTEL telescope aboard the Compton GRO [12]. The mean flux in the two ^{56}Co decay lines at 847 and 1238 keV was found to be $1.17 \pm 0.32 \pm 0.35 \times 10^{-4}$ photons cm^{-2} s^{-1} (uncertainties from statistics and systematics, respectively) [30]. When converted to ^{56}Ni mass, a best estimate of 1.5 $M_\odot$ is obtained, with a lower limit of 0.65 $M_\odot$ which accounts for uncertainties in measurement and distance to the supernova [30]. This is consistent with other estimates of SN1991Ts ^{56}Ni mass, for this peculiarly-bright event [31].

SN1998bu provided a second and seemingly better opportunity for the instruments on Compton GRO, since it exploded at a distance of 11.6 Mpc [32]. Yet, no gamma-rays from ^{56}Co decay were observed, despite a total exposure of fourteen weeks (compared to only two weeks in the case of SN1991T) [33]. The COMPTEL limit for the 1238 keV line of ^{56}Co (2.3×10^{-5} photons cm^{-2} s^{-1}) constrains the visible ^{56}Ni mass to below 0.35 $M_\odot$ if the supernova is assumed to be completely transparent to gamma-rays at the time of observations. This is probably not the case, however, and a large fraction of the γ-ray energy should be deposited in the supernova during this time window. Observations in other wavelengths suggest that 0.7–0.8 $M_\odot$ of ^{56}Ni were produced in SN1998bu [31,34]. Detailed Monte Carlo energy transport calculations show then that COMPTEL should have
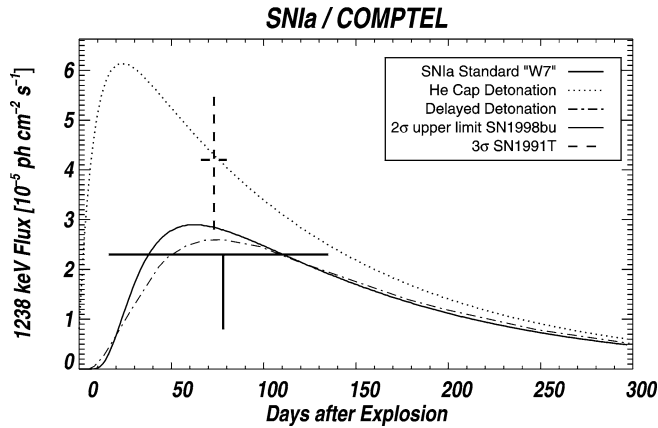
SNIa / COMPTEL

Fig. 2. Gamma-ray light curves from SNIa models, as compared to the measurements from SN1991T and SN1998bu (1238 keV line from ^{56}Co decay).

seen ^{56}Co γ-rays, at least in the framework of the "brightest" of those models (those that turn more rapidly from deflagration into detonation (W7DT) or partially-produce radioactivity in their outer ejecta (HECD) [33]).

From these two events, gamma-ray results on thermonuclear supernovae remain puzzling (see Fig. 2). Simulations show that even when γ-ray spectra can be measured with high accuracy, probably an event distance well below 10 Mpc is needed for a convincing classification of the explosion type [35].

Core collapse supernovae   In the case of ccSNe, the characteristic ^{56}Co decay γ-ray lines have been unambiguously observed in the relatively nearby (distance $\sim$ 55 kpc) SN1987A, both with the low-resolution NaI detector aboard the Solar maximum mission (SMM) [10], as with a balloon-borne Ge detector [9]; the latter showed the line to be slightly red-shifted and broadened, a fact that has not received a convincing explanation yet (see, e.g., [36]). A few years later, the OSSE instrument aboard the Compton GRO detected the 122 keV line from the decay of ^{57}Co [11], and probed further the physical conditions in the innermost exploding layers of the supernova [37].

Another important diagnostics of core-collapse supernovae is provided by ^{44}Ti, the parent isotope of the stable and abundant in nature ^{44}Ca [41]. The most plausible cosmic environment for ^{44}Ti production is the α-rich freeze-out from high-temperature burning near nuclear statistical equilibrium, or from silicon burning (e.g., [42]). Both processes occur in the innermost layers of core-collapse supernovae, which are thought to synthesize substantial amounts of ^{44}Ti, along with $\sim$1000 times more ^{56}Ni (see Fig. 5). The discovery of ^{44}Ti decay products in presolar grains [43], and the modelling of the late bolometric light curve of SN1987A with energy input from ^{44}Ti radioactivity [44] provide support to those ideas.

The lightcurve of SN1987A has been observed in unique detail for more than 15 years. After decay of the initial ^{56}Ni and ^{56}Co it appears now powered by ^{44}Ti radioactivity. The amount of ^{44}Ti is estimated to $1–2 \times 10^{-4}$ $M_{\odot}$, from recent modeling of radioactive energy
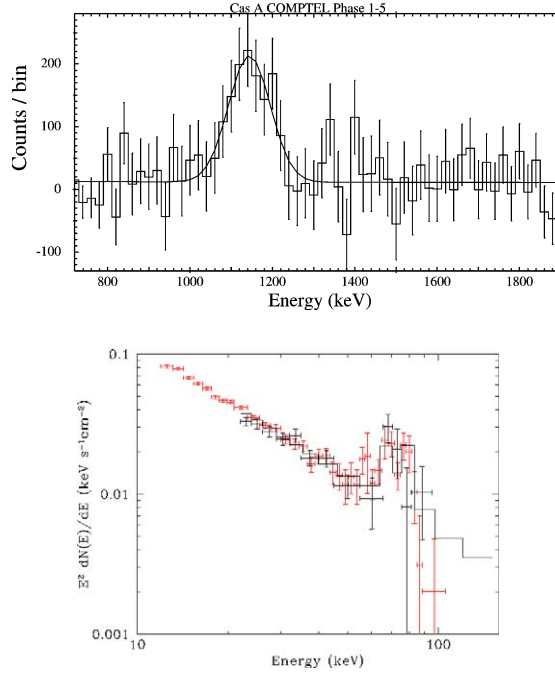
Fig. 3. Cas A supernova remnant ^{44}Ti measurements from (left) the COMPTEL instrument (1156 keV γ-ray line [38]) and from (right) the BeppoSAX (red) and INTEGRAL/IBIS (black) instruments (68 and 78 keV γ-ray lines [39,40]). (For interpretation of the references to colour in this figure legend, the reader is referred to the web version of this article.)

deposition and photon transport in the SNR [44,45]. From infrared observations, an even tighter upper limit of 1.1×10^{-4} $M_\odot$ has been derived [46]. Gamma-ray detection and proof of this interpretation is still lacking; this would be most direct. Unfortunately, the derived amount of ^{44}Ti and the distance of SN1987A result in a γ-ray line flux slightly below INTEGRALs sensitivity [45].

The 1.156 MeV γ-rays following ^{44}Ti decay have been detected in the 340 year old Galactic supernova remnant Cas A [13], at a distance of $\sim$3.4 kpc (Fig. 3). The analysis of the data cumulated by COMPTEL over the years shows that the detection is clearly significant ($> 5\sigma$), although the initially reported flux was too high, and a value of 3.4×10^{-5} photons cm^{-2} s^{-1} has been assessed [14]. A few other attempts to confirm this discovery did not succeed due to strong instrumental backgrounds (see Fig. 4). The BeppoSAX instrument has obtained a significant and convincing measurement of the low energy lines from the ^{44}Ti decay chain at 68 and 78 keV, respectively [39]. Their combined flux (at 3.4σ significance) is quoted as 1.9 and 3.2×10^{-5} photons cm^{-2} s^{-1}, for two different assumptions about the underlying continuum. Varying in spectral shape between a simple power-law and a steepening bremsstrahlung spectrum, this continuum constitutes a major systematic uncertainty of all these measurements. The results from different instruments show overall uncertainties on the order of 30–50%, so that a flux value of $2.5 \pm 1 \times 10^{-5}$ photons cm^{-2} s^{-1} is suggested (Fig. 4). Note that ^{44}Ti decays through electron
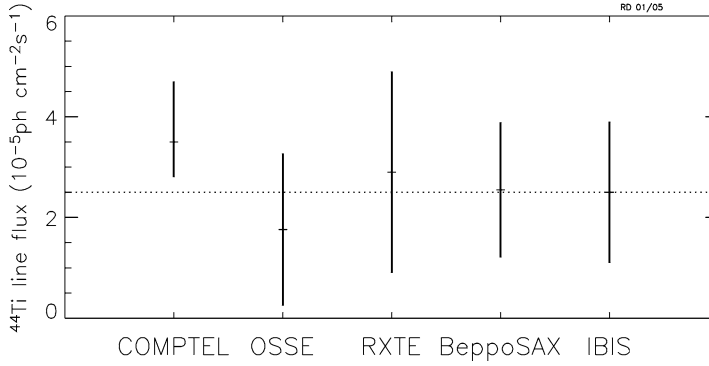
Fig. 4. Intensity measurements from different experiments for ^{44}Ti decay emission from Cas A [14,39,48,49]. (For COMPTEL and BeppoSAX, systematic uncertainty from a possible underlying continuum has been added quadratically to the statistical uncertainty.) A flux value of 2.5×10^{-5} photons cm^{-2} s^{-1} appears reasonable and corresponds to 1.5×10^{-4} $M_\odot$) of ^{44}Ti.

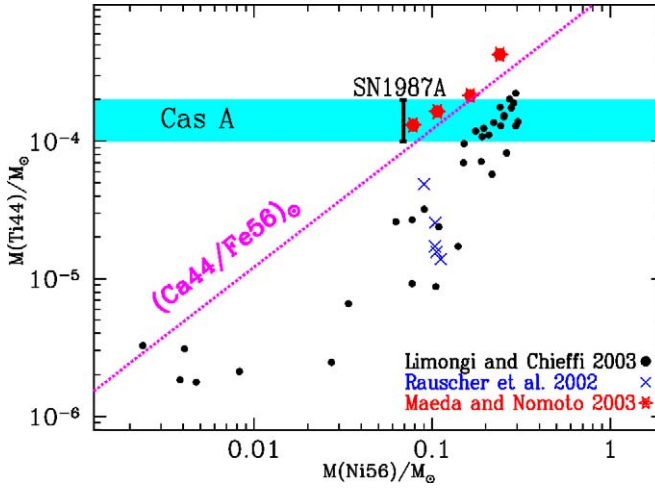

Fig. 5. Yield of ^{44}Ti vs. yield of ^{56}Ni, from models and observations. Model results are from Limongi and Chieffi (2003, filled dots, with large variations in yields due to variations in both stellar mass—from 15 to 35 $M_\odot$—and explosion energy), Rauscher et al. (2002, crosses, for stars in the 15 to 25 $M_\odot$ range and explosion energies of 10^{51} ergs) and Maeda and Nomoto (2003, asterisks); the latter concern axisymmetric explosions in 25 and 40 $M_\odot$ stars, producing high ^{44}Ti/^{56}Ni ratios. ^{44}Ti detected in Cas A appears as a horizontal shaded band (assuming that its decay rate has not been affected by ionisation in the Cas A remnant, otherwise its abundance should be lower, according to Motizuki et al. 1999). The amount of ^{44}Ti in SN1987A is derived from its late optical lightcurve (Motizuki and Kumagai 2003, see Fig. 4). The diagonal dotted line indicates the solar ratio of the corresponding stable isotopes (^{44}Ca/^{56}Fe)$_\odot$ from [5].

capture, which is considerably slowed down in ionised media. Our poor knowledge of the ionization state of ^{44}Ti in the young supernova remnant adds further uncertainty to the derived yield [47]; recent model studies obtain values similar to the case of SN1987A, i.e., in the range $1–2 \times 10^{-4}$ $M_\odot$ (Fig. 5).

The ejection of ^{56}Ni and ^{44}Ti from the inner regions of a ccSNe depends critically on the kinetic energy and the mechanism of the explosion. A substantial amount of the elements synthesized in the innermost layers may fall back onto the compact remnant. As the supernova explosion is not yet understood in sufficient detail for quantitative modeling, current studies of supernova nucleosynthesis adopt parametric descriptions: either the supernova explosion energy is injected as thermal energy at the inner boundary, or a mechanical "piston" is assumed to impart the kinetic energy of the explosion to the ejecta [19,21]. Due to these uncertainties, model yields suffer from large uncertainties, in particular for ^{44}Ti which is mostly produced near or even inside the mass cut (see Fig. 1). Kinetic energies of the explosion have been estimated as 1.2 and 2×10^{51} erg for SN1987A and Cas A, respectively [50,51]; taken at face value, those numbers suggest that more ^{44}Ti and ^{56}Ni should have been ejected in Cas A than in SN1987A. Since the peak SN luminosity is proportional to the ^{56}Ni yield, it is then rather surprising that the explosion of Cas A at only 3.4 kpc distance was not reported by contemporaneous observers around year 1671 [52]. Occultation of the Cas A supernova by circumstellar dust, which was then destroyed by the supernova blast wave, was suggested [53]. Baring this and other more exotic solutions, one concludes that the ejected ^{56}Ni amount was not overly high and rather less than the 0.07 $M_\odot$ estimated for SN1987A. Still, Cas A must have produced a rather high ^{44}Ti yield, in view of the gamma-ray observations. This is at odds with one-dimensional models for ccSN nucleosynthesis (see Fig. 1).

Another approach to estimate ^{44}Ti yields for the average ccSN is based on standard cosmic abundances, which should be reproduced by models of galactic chemical evolution that use the same model yields as those probed by gamma-rays. For that purpose, it is noted that about half of solar ^{44}Ca is produced as ^{44}Ti in ccSNe, which also produce about half of solar ^{56}Fe as ^{56}Ni (the other half coming from thermonuclear SN). It is expected then that in ccSNe the ratio of the unstable parent nuclei ^{44}Ti/^{56}Ni should match the solar ratio of the corresponding stable daughter nuclei (^{44}Ca/^{56}Fe)$_\odot \sim 10^{-3}$. However, recent supernova nucleosynthesis calculations obtain ^{44}Ti/^{56}Ni values ~ 3 times lower than that (Fig. 5). Taken at face value, this result implies that such explosions cannot produce the solar ^{44}Ca, otherwise ^{56}Fe would be overproduced [54].

Obviously, higher ^{44}Ti/^{56}Ni ratios are required from stellar models in order to satisfy the requirements of galactic chemical evolution, and such high ratios are also required to explain the high value of the ^{44}Ti yields in SN1987A and Cas A.

An exciting possibility to simultaneously solve those problems arises from the potentially important role of asymmetric explosions—this could provide the necessary boost in ^{44}Ti yields. Multi-dimensional models of supernova nucleosynthesis are difficult and computationally challenging at present. Still, preliminary parametric calculations indicate that ^{44}Ti production can be increased substantially through such asymmetries, ejecting more mass in polar regions of a rotating star during the explosion [55,56] (see Fig. 5). It remains to be shown that such models can satisfy the constraints of the standard abundance distribution for other elements, such as, e.g., the isotope ratios of Ni.

Both in Cas A and SN1987A, preferred directions are evident. The bright rings seen in SN1987As remnant suggest that rotation must have been high in the pre-supernova star to produce such torus-like dense gas during the pre-supernova wind phase [157]. Further evidence is provided by polarisation measurements [57]. In the case of Cas A, fast-moving

knots of ejecta within a standard-expanding remnant had been reported early on [58]. Early indications for a jet from optical data [59] have recently been confirmed with Chandra [60], where silicon-rich jet structures in opposite directions have been imaged in characteristic X-rays. Therefore, the diagnosis of the dynamics of ^{44}Ti ejection in Cas A, expected from deep INTEGRAL observations, promises interesting insights to this exciting problem.

Statistical constraints on the ^{44}Ti yields of supernovae can be obtained through surveys of the Milky Way and search for ^{44}Ti emission from young SN remnants (like Cas A, or younger); indeed, taking into account the estimated SN rate in the Galaxy (about 2–3 core collapse SN per century), one expects that a few of them should be detectable with present day instruments. COMPTELs survey in the 1.156 MeV band of ^{44}Ti emission is still the most complete one [61,62]. Apart from the clearly detected Cas A, a couple of candidates at low significance have been discussed (most prominently GRO J0852-4642 in the Vela region [63], and a weak signal from the Per OB2 association [61]). First INTE-GRAL results cast some doubts on the COMPTEL source of ^{44}Ti in the Vela region [64], although its spatial coincidence with a newly-discovered and rather nearby ($\leqslant 1$ kpc) X-ray SNR has led to interesting speculations about a very nearby supernova event [65]. Apparently, no bright young ^{44}Ti emitting supernova remnants are found in the inner regions of the Galaxy. Although marginally consistent with the uncertainties of such low-number statistics, it appears as if the ejection of "average" amounts of ^{44}Ti is not common in core-collapse supernovae. Monte Carlo simulations and their normalizations to COMPTEL data and to historic records of supernova observations of the last millennium [66] suggest that a rather rare supernova type with high ^{44}Ti yield is favoured by the absence of a ^{44}Ti signal from the inner Galaxy. Similar conclusions are reached by preliminary INTEGRAL data analysis [67].

3.2. Positrons, ^{22}Na and ^{7}Be from novae

Nova explosions are the result of accretion of a critical mass of H-rich material on the surface of a white dwarf in a close binary system, which leads to a thermonuclear runaway. Explosive H-burning via the hot CNO-cycle produces several radioactive species, which decay emitting gamma-rays and positrons [151].

Positrons emitted from the short-lived isotopes ^{13}N and ^{18}F annihilate with electrons inside the nova envelope and produce a prompt γ-ray emission, which appears very early (before optical maximum), lasts for $\sim$2 days and consists of a 511 keV line and a contin-uum between 20 and 511 keV. The decay of the long lived ^{7}Be and ^{22}Na produce γ-ray lines at 478 and 1275 keV, respectively (see Table 1). ^{7}Be is produced by ^{4}He $+ ^{3}$He in clas-sical CO nova (i.e., with a white dwarf composed of C and O) while ^{22}Na is produced in the hot Ne–Na cycle which occurs in ONeMg novae (with a heavier white dwarf, resulting from the evolution of 6–9 $M_\odot$ stars). Thus, the detection of the characteristic γ-ray lines of ^{7}Be and ^{22}Na would allow to unambiguously identify the composition of the progenitor white dwarf of the nova system. On the other hand a (serendipitous!) detection of the early 511 keV emission would give invaluable information on the explosion itself and the degree of mixing of the H-burning products in the envelope. Finally, ONeMg nova may also pro-duce interesting amounts of ^{26}Al; however, the COMPTEL sky map of 1.8 MeV emission
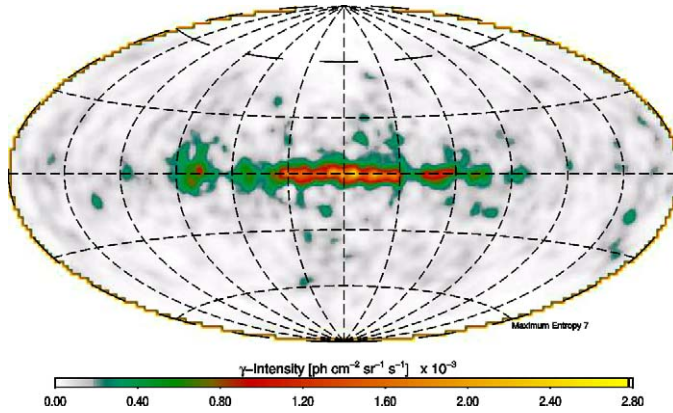
Fig. 6. All-sky image of ^{26}Al gamma-ray emission at 1809 keV as derived from COMPTELs 9-year survey [8].

in the Milky Way strongly argues for massive stars as the main source of galactic ^{26}Al (see next section).

Current nova models (with 1D hydrodynamics) are quite successful in explaining several observed propreties, like light curves, abundances and velocities of the ejecta [68,69]. However, they also suffer from uncertainties related in particular to the amount of mass ejected, which is systematically found to be lower than observed by factors ~ 10; indeed, nova models predict ejected masses of $\sim 10^{-5}$ $M_\odot$, while observations suggest values closer to $\sim 10^{-4}$ $M_\odot$. This uncertainty is reflected in the predicted intensities of the 478 and 1275 keV line and to the maximum distances for a nova explosion to be detectable by a given instrument.

Sky surveys of the 478 keV line (with the GRS instrument aboard the SMM satellite [70] and of the 1275 keV line (with GRS on SMM and with COMPTEL aboard CGRO [148] have provided only upper limits to the corresponding fluxes. These are fully compatible with current nova models [71] which predict fluxes of 2×10^{-6} photons cm^{-2} s^{-1} and 2×10^{-5} photons cm^{-2} s^{-1} for the ^{7}Be and ^{22}Na lines, respectively, for novae at a distance of 1 kpc. In view of the sensitivity of the SPI instrument aboard INTEGRAL, the maximum distances for a nova to be detectable are ~ 0.5 kpc and ~ 2 kpc, for the ^{7}Be and ^{22}Na lines, respectively. Taking into account the observed frequency of novae closer than those limits, it is expected that one such explosion will be detected by INTEGRAL in the next few years [150].

3.3. ^{26}Al and ^{60}Fe: large-scale galactic nucleosynthesis

The COMPTEL sky survey over nine years had convincingly confirmed the spectacular discovery of live ^{26}Al in the interstellar medium by the HEAO-C instrument [72]. With its imaging capability, COMPTEL had mapped structured ^{26}Al emission, extended along the plane of the Galaxy [6,8,73,74] (see Fig. 6), in broad agreement with earlier expectations [75,76]. Models of ^{26}Al emission from the Galaxy and specific localized source regions have been based on knowledge about the massive-star populations, and suggest that such stars indeed dominate ^{26}Al production in the Galaxy [7,77,78]. Galactic rota-
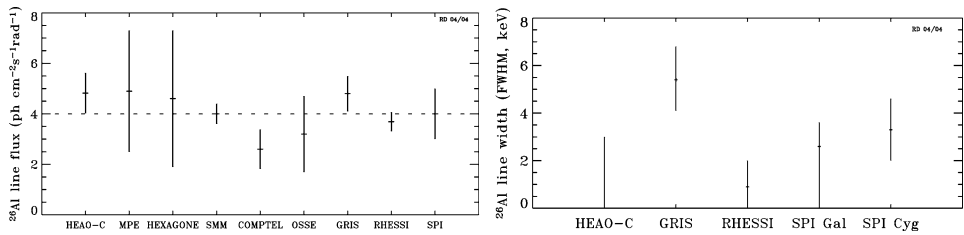
Fig. 7. Intensity measurements (left) and line width measurements (right) from different experiments for ^{26}Al emission from the inner Galaxy, and for Cygnus (rightmost datapoint).
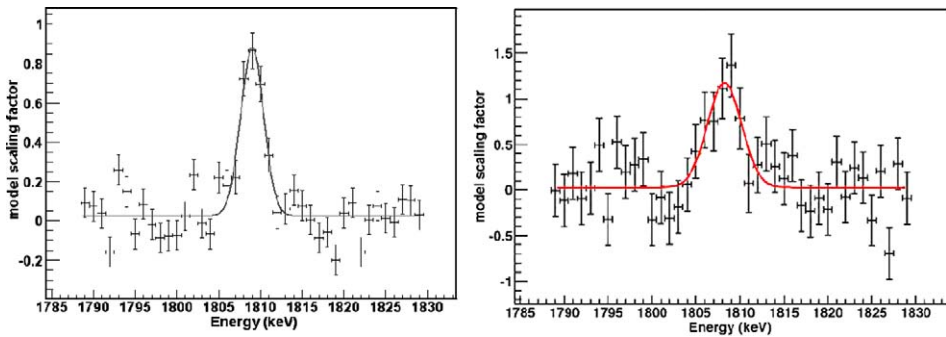

Fig. 8. SPI ^{26}Al line spectra for the inner Galaxy (left) and the Cygnus region (right). The spectra are derived by fitting skymap intensities per energy bin. Exposures are $\simeq 4$ Ms each, from the Core Program inner-Galaxy survey, and from Cygnus region calibrations and open-program data.

tion and dynamics of the ^{26}Al gas ejected into the interstellar medium are expected to leave characteristic imprints on the ^{26}Al line shape [79]. The GRIS balloon experiment carried high-resolution Ge detectors, and had obtained a significantly-broadened line [80], which translates into a kinematic (Doppler) broadening of 540 km s^{-1}. Considering the 1.04×10^6 yr decay time of ^{26}Al, such a large line width is hard to understand, and requires either kpc-sized cavities around ^{26}Al sources or major ^{26}Al condensations on grains [81,82]. Alternative measurements of the ^{26}Al line shape are then of great interest to settle this important issue.

Current results on large-scale Galactic ^{26}Al line flux and width measurements are summarized in Fig. 7. Precision follow-up measurements of 1808.7 keV emission from Galactic ^{26}Al have been one of the main science goals of the INTEGRAL mission [83]. From INTEGRAL/SPI spectral analysis of a subset of the first-year's inner-Galaxy deep exposure ("GCDE"), ^{26}Al emission was clearly detected (Fig. 8(left)) [84,85] at a significance level of 5–7σ (through fitting of adopted models for the ^{26}Al skymap to all SPI event types over an energy range $\Delta E \sim 80$ keV around the ^{26}Al line). The line width was found consistent with SPIs instrumental resolution of 3 keV (FWHM). These early SPI results are in agreement with RHESSIs recent findings [86] and do not confirm the broad ^{26}Al line reported by GRIS (Fig. 7). On the other hand, the first spectrum generated from SPI data for the Cygnus region (see Fig. 8 right for single-detector events [87]) suggests that the
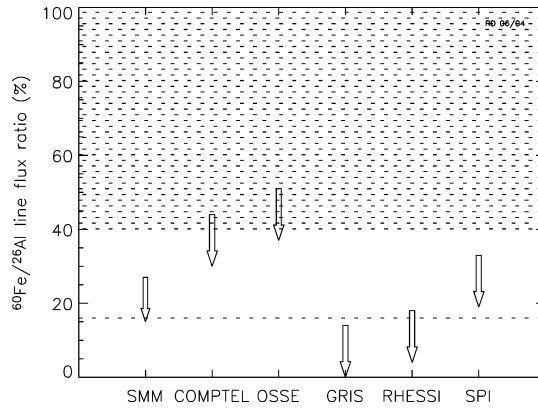
Fig. 9. Limits on the ^{60}Fe to ^{26}Al gamma-ray brightness ratio, from several experiments fall below current expectations: an often-cited theoretical value from the Santa Cruz group [54] is indicated as dotted line, the dotted area marks the regime suggested by recently-updated models, from [88]. (Note that the marginal detections by RHESSI and SPI are shown here as supper limits, based on reported uncertainties [89,159].)

line may be moderately broadened in this region. This may be caused by locally-increased interstellar turbulence from the particularly young stellar associations of Cygnus.

The detailed mapping of the Galactic distribution of ^{26}Al, obtainable through a determination of the distances to the "hot-spots" is one of the main long-term objectives of INTEGRAL [79], since it will provide the most accurate picture of recent star formation in the Milky Way [85]. On the other hand, the study of individual "hot-spots" indicated on the COMPTEL map bears on our understanding of the evolution of young stellar associations (in the cases of Cygnus, Carina and Centaurus-Circinus) and even individual stars (in the case of Vela [155]).

The fact that ^{60}Fe has not been clearly seen from the same source regions appears surprising [88], given that massive stars are expected to eject both ^{26}Al and ^{60}Fe in substantial amounts [22,54]. RHESSI reported a marginal signal (2.6σ for the combined ^{60}Fe lines at 1.173 and 1.332 MeV) [89] from the inner Galaxy, at the 10%-level of ^{26}Al brightness; SPI aboard INTEGRAL obtains a similarly low value around 10%, also at the 3σ-level [90, 159]. Obviously, ^{60}Fe γ-ray intensity from the inner Galaxy remains substantially below its ^{26}Al brightness. The situation becomes rather uncomfortable, since current nucleosynthesis models in massive stars suggest a large production of ^{60}Fe [17,22,153], substantially larger than older calculations (see [88] and references therein). This is mainly due to increased neutron capture cross sections for Fe isotopes, and a reduced ^{59}Fe β-decay rate. The expected gamma-ray line flux ratio of ^{60}Fe/^{26}Al falls between 40 and 120%, depending on how the interpolation between the few calculated stellar-mass gridpoints is done, and which of the models are taken as baseline; in comparison, the IMF choice appears uncritical. In any case, those revised expectations clearly lie above the experimental limits for Galactic ^{60}Fe emission (Fig. 9). Obviously, observations do not support predictions of current stellar nucleosynthesis (or, alternatively, they suggest that ccSNe are not the dominant sources of Galactic ^{26}Al). The answer to this interesting nucleosynthesis puzzle may be related to nuclear-physics issues, probably concerning the (uncertain) neutron capture reactions on unstable ^{59}Fe.

3.4. Positron annihilation

Ever since Anderson's discovery of the positron in 1932, the question of the existence of antimatter in the Universe has puzzled astrophysicists. Besides the production of positrons in the laboratory and by cosmic rays in our atmosphere, positrons were supposed to be produced in a multitude of astrophysical environments (e.g., [156]).

Observations   In the seventies, balloon instruments provided first evidence for e^-e^+ annihilation from the Galactic center region. As the line was discovered at an energy of 476 ± 26 keV [91], the physical process behind the emission was initially ambiguous and had to await the advent of high resolution spectrometers. In 1977, germanium semiconductors, flown for the first time on balloons, allowed to identify a narrow annihilation line at 511 keV, its width being a few keV only [92,93]. The eighties were marked by ups and downs in the measured 511 keV flux through a series of observations performed by balloon-borne germanium detectors (principally the telescopes of Bell-Sandia and Goddard Space Flight Center). Those results were interpreted as the signature of a fluctuating compact source of annihilation radiation at the Galactic center (see, e.g., [94]). Additional evidence for this scenario came initially from HEAO-3 [95] reporting variability in the period between fall 1979 and spring 1980. Yet, during the early nineties, this interpretation was more and more questioned, since neither eight years of SMM data [96] nor the revisited data of the HEAO-3 Ge detectors [97] showed evidence for variability in the 511 keV flux. Throughout the nineties, CGROs oriented scintillation spectrometer experiment (OSSE) measured steady fluxes from a Galactic bulge and disk component [15] and rough skymaps became available based on the combined data from OSSE, SMM and TGRS. The corresponding pre-INTEGRAL view of galactic positron annihilation invokes different scenarios based on two main components—a central bulge or halo and a Galactic disk [16,98]: "bulge-dominated" models comprise a halo bulge plus a thin disk, while in the "disk-dominated" scenario a 2D Gaussian bulge without a halo combines with a thick disk. The integrated annihilation rate is similar in the various models, but the data do not strongly constrain the bulge to disk flux ratio which spans a range going from $B/D = 3.3$ (bulge-dominated) to $B/D = 0.2$ (disk-dominated).

A possible third component at positive Galactic latitude (between $l = 9°$–$12°$) was first attributed to an annihilation fountain in the Galactic center [99]; however the intensity and morphology of this feature were only weekly constrained by the data [98].

Regardless of their discrepant flux estimates, pre-INTEGRAL missions were in good agreement with respect to the observed "positronium fraction" f_{Ps}, the fraction of positrons which annihilates after having formed positronium atoms. The positronium (Ps) fraction is calculated as $f_{Ps} = 2/[2.25(I_{511}/I_{Ps}) + 1.5]$ where I_{511} and I_{Ps} are the intensities in the 511 keV line and the 3-photon continuum emissions respectively. Observed Ps fractions converged towards $f_{Ps} = 0.93 \pm 0.04$ [16,100].

Since the launch of INTEGRAL in October 2002, a large part of this mission's core program has been devoted to a Galactic central region deep exposure (GCDE). Imaging analyses from data of the INTEGRAL spectrometer SPI during the first year shows the 511 keV emission to be spatially extended ($9° \pm 1°$ FWHM), however, rather symmetric and centered around the Galactic center [105–107,149,152]. The corresponding bulge flux

Table 2

The Galactic center 511 keV line measured by high resolution spectrometers

Instrument	Year	Flux [10^{-3} photons cm^{-2} s^{-1}]	Centroid [keV]	Width FWHM [keV]	Ref.
HEA03	1979–1980	1.13 ± 0.13[a]	510.92 ± 0.23	$1.6^{+0.9}_{-1.6}$	[101]
SMM	1980–1986	2.1 ± 0.4[a]		Unresolved	[102]
GRIS	1988, 1992	0.88 ± 0.07[b]		2.5 ± 0.4	[103]
HEXAGONE	1989	0.95 ± 0.23[b]	511.54 ± 0.34	2.66 ± 0.60	[104]
OSSE	1991–2000	2.4–3.1[c]		Unresolved	[160]
TGRS	1995–1997	1.07 ± 0.05[a]	511.98 ± 0.10	1.81 ± 0.54	[100]
SPI	2003	$0.96^{+0.21}_{-0.14}$[d]	$511.02^{+0.08}_{-0.09}$	$2.67^{+0.30}_{-0.33}$	[105]

[a] For a point source or spatially unresolved source at the Galactic center. [b] Galactic center flux within the instruments field of view: 18° and 19° FWHM for GRIS and HEXAGONE, respectively. [c] Best fit fluxes of a bulge and disk model—uncertainty from thin/thick disk model. [d] Best fit flux in spherical Gaussian with 8° FWHM centered the GC.

is 10^{-3} photons cm^{-2} s^{-1}, with a 15% uncertainty being dominated by the width of the Gaussian intensity distribution. Marginal evidence for emission from a Galactic disk has been found only recently [108], with an intensity which leaves little room for positrons other than the ones from ^{26}Al decay. However, a positive latitude enhancement of annihilation emission, as had been suggested from OSSE measurements, appears rather unlikely, from INTEGRALs measurements. The inner-Galaxy emission at 511 keV cannot be explained by a single source, but the contribution of a number of point sources cannot yet be excluded by SPI. Spectroscopy of 511 keV line emission from the bulge resulted in a best fit energy of $511.02^{+0.08}_{-0.09}$ keV and an intrinsic line width of 2.6 ± 0.3 keV FWHM [107,109]. A positronium continuum is detected [107,110] and contains about 3–5 times the γ-ray flux than the line itself (a Positronium fraction of 0.93 is consistently derived). Together with the detailed shape of the 511 keV line, this suggests annihilation in a warm medium [107,111,112] (Fig. 11). Annihilation in a hot medium would produce a much broader line than observed, whereas the annihilation from a cold medium after thermalization would cause a narrower line profile than observed. Also, a substantial contribution from annihilation on the surface of interstellar grains is considered unlikely, from the line peak to wing area comparisons. Hence, detailed 511 keV spectroscopy introduced a new probe of the physics of the interstellar medium in the Galactic bulge.

With its superior angular resolution and good sensitivity for point sources, INTEGRALs imager IBIS has the potential to reveal whether the extended bulge emission is of genuinely diffuse origin or results from blended emission from a number of compact sources. The analysis of INTEGRAL/ISGRI data during the first year of the missions Galactic center deep exposure [114] shows no evidence for point sources at 511 keV; the 2σ upper limit for resolved single point sources is estimated to 1.6×10^{-4} photons cm^{-2} s^{-1}.

In the near future, additional exposure and improved knowledge of background systematics will refine INTEGRALs image of Galactic e$^-$e$^+$ annihilation, and better constrain the numerous models proposed for its origin.
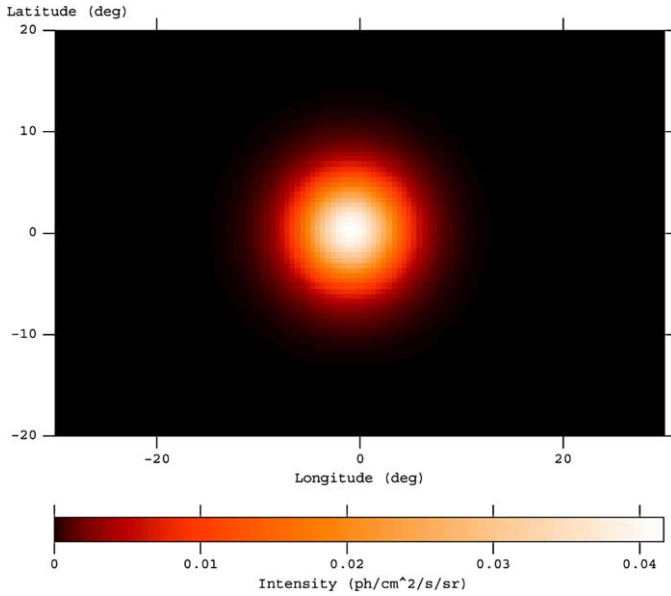
Fig. 10. INTEGRAL/SPI best fit model for the 511 keV line emission from the GC region. A Gaussian with 8° FWHM, representing the Galactic bulge, is sufficient to explain the data of the first GCDE, from [106]. Recent imaging deconvolutions through various method variants essentially confirm such a model, yet are still too limited to allow extraction of significant details beyond such a model [108].
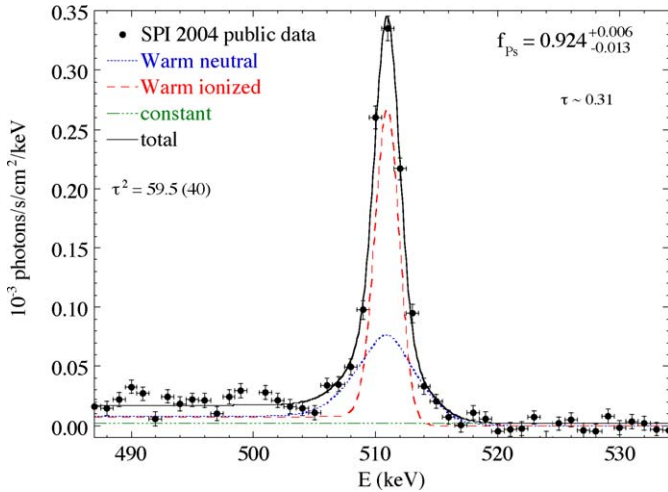

Fig. 11. INTEGRAL/SPI measurement of the shape of the 511 keV line from positron annihilation (figure courtesy [113]). Compared to expectations from annihilations in different phases of the ISM, one finds that warm ISM in its neutral and ionized parts contributes equal amounts to total annihilation, while cold and hot ISM phases appear insignificant [107,112,113].

Astrophysical models Our view of Galactic positron annihilation is considerably simplified with the SPI results: the e^-e^+ emission apparently originates from a simple 8°-wide (FWHM) central bulge, and there is not any evidence for deviations from such Galactocentric symmetry. The weakness of the disk component comes as a surprise, since positrons are necessarily produced in the galactic disk by radioactive isotopes produced in supernovae and novae. The observed ^{26}Al alone (see Section 3.3) can account for $\sim 5 \times 10^{-4}$ photons cm^{-2} s^{-1} of the disk's 511 keV γ-ray brightness, since its decay is accompanied by the emission of a positron in 85% of the cases.

INTEGRAL is therefore reformulating the question on Galactic e^-e^+ annihilation: in order to explain $\simeq 10^{-3}$ photons cm^{-2} s^{-1} in the 511 keV line at distance of the Galactic center, an annihilation rate of $\simeq 10^{43}$ positrons per second is required in a relatively small bulge region around the GC (assuming a distance of 8 kpc to the GC and a positronium fraction of $f_{Ps} = 0.94$, resulting in 0.59511 keV line photons emitted per positron annihilation).

Amongst the mechanisms that have been proposed for the origin of Galactic positrons are (a) β^+-decaying radioactive isotopes; (b) the decay of π^+'s produced in cosmic-ray proton interaction with interstellar nuclei; (c) high energy processes (e.g., pair creation by high-energy photons) in compact objects, and (d) bosonic dark matter annihilation of low mass particles (1–100 MeV) in the Galactic halo; the latter has been specificaly proposed to explain the morphology of the 511 keV emission after the first SPI measurements.

The simple morphology of the 511 keV emission observed by SPI, if conservatively interpreted, suggests that the Galaxy's old stellar population is at its origin; alternatively, something much more exotic, like dark matter, may be at work. In the following we focus on e^+ sources concentrated in the central region, and neglect ^{26}Al and cosmic ray production of positrons (which should be clearly seen in the disk).

Type Ia supernovae. The light curves of SNe Ia are powered by the deposition in the expanding SN ejecta of the gamma-rays and positrons produced by various radioactivities, especially the decay of ^{56}Co, ^{44}Ti and ^{57}Co (the latter does not release positrons). Whether the positrons escape from the ejecta or not, depends on the strength and geometry of the magnetic field. Positron transport in SNIa models was simulated [115]. It was found that, for favorable magnetic field configurations, $\sim 5\%$ of ^{56}Co decay positrons may escape the ejecta. Comparing a sample of late light curves of supernovae type Ia with simulations [116,117], the underlying idea can be tested that positron escape leads to power loss from the system and a drop in the late lightcurve. These studies conclude that the number of positrons escaping a typical SNIa is $N \sim 8^{+7}_{-4} \times 10^{52}$, or about 3% of the total amount of positrons released by ^{56}Co decay. Note that the amount of ^{44}Ti produced in SNIa is 4–5 orders of magnitude smaller than the one of ^{56}Ni [118], so that even if all the positrons released by ^{44}Ti decay escape the supernova, their contribution to the above number N is negligible.

The production rate of positrons R from SNIa in the bulge might then be estimated as $R = MFN$ [5], where M is the mass of the bulge (in units of 10^{10} $M_\odot$) and F is the SNIa frequency in a bulge-like system (expressed as number of SNe per century and per 10^{10} $M_\odot$ in stars). Adopting $M = 1.5 \pm 0.5$ [119] and $F = 0.044 \pm 0.03$ [2] a positron production rate $R \simeq 2 \times 10^{42}$ positrons per second is obtained. This figure corresponds to about 20% of the required bulge positron production rate after SPI and is twice as large as in

previous estimates (e.g., [5]), because of the recently revised SN rates of [2]. This increase with respect to previous estimates, although not solving the problem, should remind us that the uncertainties (statistical and systematic) of the various parameters entering the calculation of R may be substantially larger than formally quoted. It appears to us that current uncertainties are such that SNIa can either be major contributors to the 511 keV emission or have a negligible contribution.

On the one hand, the SNIa frequency F may still be considerably underestimated, due to dust extinction in the inner galaxian regions and to the difficulty of detecting supernovae against the bright background of stellar bulges; indeed, it is intriguing that no SNIa have been found up to now in the bulges of spirals [120]. On the other hand, the estimate of the number of positrons N by Milne et al. [117] might be too optimistic. For one well studied case, the SN Ia 2000cx, Sollerman et al. [34] find that the decay of the late optical lightcurve is accompanied by an increased importance of the near-IR emissivity and does not necessarily imply an escape of positrons from the ejecta. In the simple model of Sollerman et al. accounting for the UVOIR observations, all positrons are trapped in the ejecta. The investigation of positron escape from SNIa through the study of late lightcurves requires more observations and more realistic models. The contribution of this class of objects appears promising, but other sources should definitely be sought.

LMXB. The morphology of their distribution makes low mass X-ray binaries (LMXBs) very promising candidate sources [5]: their observed distribution in the Milky Way is strongly concentrated towards the Galactic bulge. Furthermore, the collective X-ray emissivity of Galactic LMXBs is 10^{39} erg/s [121], compared to the 10^{37} erg/s required to produce 10^{43} positrons per second. It thus is sufficient to convert only 1% of the available energy into positrons to explain the bulge emission. However, the mechanism of that conversion is not known yet.

Light–dark matter. It has been argued [122] that low mass bosonic dark matter may be the source of the observed 511 keV emission line. The dark matter particles annihilate throughout the Galactic bulge into e^-e^+ pairs which, after decelerating, annihilate into 511 keV photons. The proposed particles are quite light (in the 1–100 MeV range) so that their annihilation does not produce undesirable high energy gamma-rays, and in that respect they do not correspond to the most commonly discussed dark matter candidate, which has mass in the GeV to TeV range. Moreover, rather special properties are required for such light particles to justify why they have escaped detection up to now in accelerators such as the LEP.

Various profiles for the dark matter density have been proposed, differing vastly from each other. It is likely that the dark matter density profile is cusped as $1/r$ at small galactic radii; hence the gamma-ray flux would be expected to be considerably enhanced. Discriminating between ill-defined dark matter distributions and other bulge candidate sources (LMXB, SNIa) with INTEGRAL/SPI will be a very difficult task. More generally, it is hard to evaluate the plausibility of the dark matter hypothesis, since the required properties of the source (i.e., density profile, annihilation cross section) are completely unknown/unconstrained; in fact, the observed properties of the 511 keV emission (intensity and density profile) are used in [122] in order to derive the properties of the dark matter source of positrons.

Another method to determine whether the 511 keV line is due to dark matter annihilation is to seek a 511 keV signature from low surface brightness dwarf galaxies [123], which appear to be dark matter-dominated. If the emission line detected in our Galaxy is due to dark matter annihilation, then a relatively intense 511 keV line from nearby dwarf galaxies is also expected. For the Sagittarius dwarf galaxy, a 511 keV flux of $(1–7) \times 10^{-4}$ photons $cm^{-2} s^{-1}$ was prediced [123]. Based on the limited statistics of INTEGRAL/SPIs first year core program data, a 2σ upper limit of 2.5×10^{-4} photons $cm^{-2} s^{-1}$ on the annihilation flux from the Galaxy is set [124].

However, at this point, the non-detection of the Sagittarius dwarf galaxy can neither rule out nor confirm the light dark matter hypothesis. Only with deeper exposure of dark matter targets (such as Sagittarius or the globular cluster Palomar-13), SPI/INTEGRAL will reach adequate sensitivity to effectively reject or confirm light dark matter annihilation as source of the bulge 511 keV emission.

3.5. Nuclear de-excitation lines: He isotopic abundances in the Sun, and particle acceleration physics

Cosmic rays and high-energy γ-rays from active galactic nuclei (AGN), supernova remnants, and the Galactic interstellar medium demonstrate the existence of efficient particle accelerators in the universe [125,126]. Although it is generally believed that Fermi acceleration is the only mechanism capable to provide the observed particle energies, the acceleration process, and the associated injection of suprathermal particles into the acceleration region, is far from being understood. Energetic particles produce characteristic γ-rays from nuclear de-excitation upon their collisions with ambient matter.

The Sun is our closest laboratory for the study of energetic particles. Within the Solar system, solar energetic particles can even be directly measured through particle detectors in interplanetary space [127], although their interpretation is complex due to modulation from local magnetic fields. Characteristic γ-ray emission is produced when solar flare events produce a burst of energetic particles, which collides with gas of the upper solar atmosphere.

Detailed measurements of γ-ray flare spectra have been obtained by the Compton Observatory at rather modest resolution [128], and more recently with Ge-detector resolution by the RHESSI experiment [129]. Such spectra exhibit complex superpositions of narrow solar-atmosphere and broad solar-flare particle de-excitation lines, often buried in an intense electron bremsstrahlung continuum [128]. There is correlated and slower variability of lines originating from neutron interactions, as compared to other nuclear deexcitation lines. This difference between lines caused by high-energy proton spallations as compared to lines caused by low-energy proton collisions and to bremsstrahlung from flare electrons suggests different acceleration sites for the high- and low-energy particles which hit solar atmosphere material in such flares: Fermi acceleration initiated by large-scale processes in the solar magnetosphere may lead to very energetic solar-flare particles, far beyond electrostatic or Fermi accelerators set up by more rapid loop reconnection events in the loop structures, which provide the electron and low-energy particle components [130].

With RHESSIs high spectral resolution, specific γ-ray lines could be studied in much more detail, investigating nuclear-physics processes.

The positron annihilation line at 511 keV provides a unique opportunity to investigate how positron annihilation proceeds: positrons are produced at high energies, both from nuclear interactions and from radio-isotopes produced through spallation reactions. Thermalization mostly precedes annihilation, which then can occur on bound electrons to produce a rather narrow line (FWHM $\simeq$ 1.5 keV), while annihilation through formation of positronium atoms not only produces the triplet-state continuum spectrum below 511 keV, but also a rather broad 511 keV line (FWHM $\simeq$ 6–7 keV) [131,132]. If annihilation occurs before thermalization, or else in a hot environment, also the charge exchange reaction channel may produce a broader line. In this respect, RHESSIs findings are puzzling [133]: The measured broad line would suggest annihilation through Positronium formation, but the line-to-annihilation-continuum ratio is inconsistent with this explanation; on the other hand, a thermal interpretation of the broad line violates the sequence of thermalization and charge-exchange annihilation, because it suggests annihilation high up in the solar atmosphere, well above the positron production region.

In impulsive solar flares, isotopic enrichment of ^{3}He up to $\simeq$ 4 orders of magnitude above the ratio in solar wind of 5×10^{-4} has been observed; this is much discussed, especially in terms of isotopically-selective particle acceleration. The reaction ^{16}O(^{3}He, p)^{18}F* produces characteristic γ-ray lines at 937, 1042, and 1081 keV, which allows ^{3}He abundance determination through solar flare γ-ray spectra [134]. From SMM and CGRO flare γ-ray spectra, flare-averaged ^{3}He/^{4}He abundance ratios between 0.1 and 1 have been deduced in this way [135]. However, uncertainties from the above reaction rate and its energy dependence are a concern [136].

The geometry of the accelerated-particle beam is reflected in a variety of γ-ray line parameters: RHESSIs high imaging resolution through a rotating modulation collimator allowed imaging in the 2.223 MeV neutron capture line, finding it offset from the source of X-ray bremsstrahlung continuum [137,154]; this suggests that the flare particles hit the solar atmosphere at an angle and not perpendicularly. RHESSI and SPI found significant redshifts in γ-ray lines from C, O, Ne, Mg, Si, and Fe [138,139], which suggest downward-beamed nuclei being responsible for the emission. ^{7}Be and ^{7}Li lines at 429 and 478 keV, respectively, from collisions of flare and ambient α nuclei are, however, so broad that isotropic rather than beamed energetic α-particles must be assumed [133].

Evidently, more RHESSI flare γ-ray observations will be necessary to obtain a more consistent picture on particle acceleration in solar flares.

The complexity of nuclear de-excitation line γ-ray spectra is expected to be greatly simplified in the "thin-target" configuration, which presumably is realized when low-energy cosmic rays collide with ambient matter in star-forming regions and the general interstellar medium [140]. The COMPTEL discovery of intense nuclear de-excitation γ-rays [141] came as a surprise and provided a great stimulus to studies of low-energy cosmic rays; the experimenters withdrew their discovery however, when they noted that instrumental background may have caused such a signal artifact [142]. Thus, nuclear lines from cosmic ray interactions still are to be discovered. Predicted intensities [143] of $\simeq 10^{-6}$ photons cm^{-2} s^{-1} leave little hope for INTEGRAL.

4. Summary and perspectives

Despite the serious handicaps of a rather modest spatial resolution and signal/noise ratios in the percent regime, astronomy with gamma-ray lines became a major discipline of modern astrophysics in the 90ies. In particular, this branch of astrophysics provides unique views to:

- the interiors of supernovae, through measurements of ^{56}Co and ^{57}Co as detected in SN1987A, and of ^{44}Ti as detected in Cas A;
- the current large-scale star formation and massive-star/ISM interactions in the Milky Way, through mapping and spectroscopy of ^{26}Al in the Galaxy;
- stellar nucleosynthesis, through the constraints imposed by the abundance ratios of ^{44}Ti/^{56}Co and ^{26}Al/^{60}Fe;
- the source (and, perhaps, propagation) of positrons in the Galaxy, through the intensity and morphology of the 511 keV line, as mapped by SPI/INTEGRAL.

Those important results have lead to several new questions:

- What fraction of radioactive energy is converted into other forms of energy in supernovae? (The issues are: What is the absolute amount of (presently indirectly-inferred) radioactive ^{56}Ni in SNIa, and of ^{44}Ti in core-collapse SNe; what is the magnitude of positron leakage from supernovae; is the morphology of expanding supernova envelopes dominated by inhomogeneities, "bullets", filaments, jets, magnetic fields?)
- How good are our (basically one-dimensional) models for nova and supernova nucleosynthesis, in view of important 3D effects such as rotation and convective mixing? (The issues are: How much ^{44}Ti mass can in principle be (and is effectively) ejected from regions near the mass cut between compact remnant and ejected supernova envelope; how realistic are nova ^{22}Na yields, what are the ejected nova-envelope masses, how critical are the seed compositions for explosive hydrogen burning in novae.)
- What is the dynamic range of physical conditions expected for nucleosynthesis events? (The issues are: How does nucleosynthesis vary with stellar mass and metallicity, what are the applicable supernova rates in specific ensembles of massive stars; how much clustering of events is there in space and time; does self-enrichment play a major role; is star formation triggered in dense, active nucleosynthesis regions.)
- What is the interplay between interstellar medium and energy outputs and material ejecta from massive stars? (The issues are: Which are the characteristic temporal and spatial scales of energy and material flows in interstellar gas; how does the morphology of the interstellar medium affect such scales; do lower and higher mass stars form at special epochs and locations; where are the presolar grains formed, and how are they processed before we detect them in the meteoritic laboratory?)
- How do positrons end up annihilating to produce γ-ray photons? (The issues are: How do they escape their sources, how do they propagate through interstellar space and possibly the Galactic halo; what are the resulting slowing down times, and their total lifetimes before annihilation, and what is its spread; what is the final annihilation en-

vironment, and how localized does annihilation occur; what is the ratio between the different sources of nucleosynthesis, compact stars, and possibly dark matter?)

- How are particles accelerated to cosmic-ray energies? (The issues are: Which isotopes are selectively injected into the acceleration region; how does "injection" occur, from thermalized seed particles; which magnetic-field configuration sets up accelerators at different sites and on different scales; how do these accelerators shape the isotopic composition; which secondary isotopes are produced by cosmic ray spallation reactions; where and how is spallation nucleosynthesis most efficient; what is the role of compact stars and their accretion?)

With the INTEGRAL [83,144,145] and RHESSI [146] space experiments, now the new step is taken with high-resolution spectrometers, improving sensitivities by $\simeq$ an order of magnitude through the use of large volumes of Ge detectors. More importantly, with these instruments we now can observe kinematic signatures from Doppler-shifted energy values in expanding/accelerated radioactive material and in positron annihilations in interstellar space through different reaction channels. With such measurements, new valuable constraints are being obtained on sources of cosmic nucleosynthesis.

References

[1] F. Matteucci, A. Renda, A. Pipino, M. Della Valle, Astron. Astrophys. 405 (2003) 23.
[2] F. Mannucci, et al., astro-ph/0411450.
[3] R. Diehl, et al. (Eds.), Special Issue of New Astron. Rev. 48 (1–4) (2004).
[4] R. Diehl, F.X. Timmes, Publ. Astron. Soc. Pac. 110 (748) (1998) 637.
[5] N. Prantzos, ESA SP 552 (2004) 15.
[6] R. Diehl, C. Dupraz, K. Bennett, et al., Astron. Astrophys. 298 (1995) 445.
[7] N. Prantzos, R. Diehl, Phys. Rep. 267 (1996) 1.
[8] S. Plüschke, R. Diehl, V. Schönfelder, et al., ESA SP 459 (2001) 55.
[9] J. Tueller, S. Barthelmy, N. Gehrels, et al., Astrophys. J. 351 (1990) L41.
[10] S. Matz, G.J. Share, M.D. Leising, et al., Nature 331 (1988) 416.
[11] J.D. Kurfess, W.N. Johnson, R.L. Kinzer, et al., Astrophys. J. Lett. 399 (1992) L137.
[12] D. Morris, et al., AIP Conf. Proc. 410 (1997) 1087.
[13] A.F. Iyudin, R. Diehl, H. Bloemen, et al., Astron. Astrophys. 284 (1994) L1.
[14] V. Schönfelder, H. Bloemen, W. Collmar, et al., AIP Conf. Proc. 510 (2000) 54.
[15] W.R. Purcell, L.-X. Cheng, D.D. Dixon, et al., Astrophys. J. 491 (1997) 725.
[16] R. Kinzer, et al., Astrophys. J. 559 (1999) 705.
[17] T. Rauscher, et al., Astrophys. J. 576 (2002) 323.
[18] A. Palacios, et al., Astron. Astrophys. 429 (2005) 613.
[19] S.E. Woosley, T.A. Weaver, Astrophys. J. Suppl. 181 (1995) 101.
[20] A. Chieffi, M. Limongi, Publ. Astron. Soc. Austral. 20 (2003) 324.
[21] F.K. Thielemann, et al., Astrophys. J. 460 (1996) 408.
[22] M. Limongi, A. Chieffi, astro-ph/0411441, Nucl. Phys (2005), in press.
[23] H.-T. Janka, et al., in: W. Hillebrandt, B. Leibundgut (Eds.), From Twilight to Highlight: The Physics of Supernovae, Springer, Berlin, 2003, p. 39.
[24] D.W. Arnett, Astrophys. J. 157 (1969) 1369.
[25] M. Hamuy, Astrophys. J. 582 (2003) 905.
[26] W. Hillebrandt, in: J.M. Marcaide, E. Weiler (Eds.), Cosmic Explosions, Springer, Berlin, 2004, p. 241.
[27] K. Nomoto, F.-K. Thielemann, K. Yokoi, Astrophys. J. 286 (1984) 644.
[28] P. Höflich, A. Khokhlov, Astrophys. J. 457 (1996) 500.

[29] P. Höflich, et al., Astrophys. J. 568 (2002) 791.
[30] D. Morris, et al., unpublished, Morris died from cancer in 2003, Astrophys. J. (2002) submitted for publication.
[31] B. Leibundgut, Astron. Astrophys. Rev. 10 (2000) 179.
[32] J. Hjorth, N.R. Tanvir, Astrophys. J. 482 (1997) 68.
[33] R. Georgii, et al., Astron. Astrophys. 394 (2002) 517.
[34] J. Sollerman, Astron. Astrophys. 428 (2004) 555.
[35] J. Isern, et al., New Astron. Rev. 48 (1–4) (2004) 31.
[36] K.J. Grant, A.J. Dean, Astron. Astrophys. Suppl. 97 (1993) 211.
[37] D.D. Clayton, et al., Astrophys. J. 399 (1992) L141.
[38] A.F. Iyudin, R. Diehl, H. Bloemen, et al., ESA SP 382 (1997) 37.
[39] J. Vink, et al., Astrophys. J. 560 (2001) L79.
[40] J. Vink, Sp. Sci. Rev. (2005), in press.
[41] S.E. Woosley, W.D. Arnett, D.D. Clayton, Astrophys. J. Suppl. 26 (1973) 231.
[42] D.W. Arnett, Supernovae and Nucleosynthesis, Princeton Univ. Press, Princeton, NJ, 1996.
[43] L.R. Nittler, S. Amari, E. Zinner, S.E. Woosley, R.S. Lewis, Astrophys. J. 462 (1996) L31.
[44] C. Fransson, C. Kozma, New Astron. Rev. 46 (2002) 8–10.
[45] Y. Mochizuki, S. Kumagai, New Astron. Rev. 48 (2004) 69.
[46] P. Lundqvist, C. Kozma, J. Sollerman, C. Fransson, Astron. Astrophys. 374 (2001) 629.
[47] Y. Mochizuki, K. Takahashi, H.-Th. Janka, W. Hillebrandt, R. Diehl, Astron. Astrophys. 346 (1999) 831.
[48] L.-S. The, et al., Astron. Astrophys. Suppl. 120 (1996) 357.
[49] R. Rothschild, et al., Nucl. Phys. B 69 (1–3) (1998) 68.
[50] M.D. Laming, U. Hwang, Astrophys. J. 597 (2003) 347.
[51] V.P. Utrobin, Astron. Lett. 50 (5) (2004) 293.
[52] J.R. Thorstensen, R.A. Fesen, S. van den Bergh, Astron. J. 122 (2001) 297.
[53] J. Schmidt, P. Predehl, Astron. Astrophys. 293 (1995) 889.
[54] F.X. Timmes, S.E. Woosley, D.H. Hartmann, et al., Astrophys. J. 464 (1996) 332.
[55] S. Nagataki, et al., Astrophys. J. 486 (1997) 1026.
[56] K. Maeda, K. Nomoto, Astrophys. J. 598 (2003) 1163.
[57] L. Wang, J.C. Wheeler, P. Hoeffich, et al., Astrophys. J. 579 (2002) 671.
[58] R.A. Fesen, R.H. Becker, W.P. Blair, Astrophys. J. 313 (1987) 378.
[59] R.A. Fesen, K.S. Gundersen, Astrophys. J. 470 (1996) 967.
[60] U. Hwang, et al., Astrophys. J. 615 (2004) L117.
[61] C. Dupraz, et al., Astron. Astrophys. 324 (1997) 683.
[62] A.F. Iyudin, et al., Astrophys. Lett. Commun. 38 (1998) 383.
[63] A.F. Iyudin, et al., Nature 369 (1998) 140.
[64] A. von Kienlin, D. Attie, S. Schanne, et al., ESA SP 552 (2004) 87.
[65] B. Aschenbach, A.F. Iyudin, V. Schönfelder, Astron. Astrophys. 350 (1999) 997.
[66] L.-S. The, et al., AIP Conf. Proc. 510 (2000) 64.
[67] M. Renaud, F. Lebrun, J. Ballet, et al., ESA SP 552 (2004) 81.
[68] M. Hernanz, et al., Astrophys. J. 526 (1999) L97.
[69] S. Starrfield, et al., Mon. Not. R. Astron. Soc. 296 (1998) 502.
[70] M.J. Harris, M.D. Leising, G.H. Share, Astrophys. J. 375 (1991) 216.
[71] J. Jose, A. Coc, M. Hernanz, Astrophys. J. 520 (1999) 347.
[72] W.A. Mahoney, J.C. Ling, A.S. Jacobson, R.E. Lingenfelter, Astrophys. J. 262 (1982) 742.
[73] J. Knödlseder, D. Dixon, K. Bennett, et al., Astron. Astrophys. 345 (1999) 813.
[74] U. Oberlack, Ph.D. Thesis, Technische Universität München, 1997.
[75] N. Prantzos, in: Ph. Durouchoux, N. Prantzos (Eds.), Gamma-Ray Line Astrophysics, AIP, New York, 1991, p. 129.
[76] N. Prantzos, Astrophys. J. 405 (1993) L55.
[77] J. Knödlseder, K. Bennett, H. Bloemen, et al., Astron. Astrophys. 344 (1999) 68.
[78] J. Knödlseder, Astrophys. J. 510 (1999) 915.
[79] K. Kretschmer, R. Diehl, D.H. Hartmann, Astron. Astrophys. 412 (2003) 47.
[80] J.E. Naya, S.D. Barthelmy, L.M. Bartlett, et al., Nature 384 (1996) 44.

[81] W. Chen, R. Diehl, N. Gehrels, et al., ESA SP 382 (1997) 105.
[82] S.J. Sturner, J.E. Naya, Astrophys. J. 526 (1999) 200.
[83] C. Winkler, T.J.-L. Courvoisier, G. Di Cocco, Astron. Astrophys. 411 (2003) L1.
[84] R. Diehl, J. Knödlseder, G.G. Lichti, et al., Astron. Astrophys. 411 (2003) L451.
[85] R. Diehl, K. Kretschmer, G.G. Lichti, et al., ESA SP 552 (2004) 27.
[86] D. Smith, Astrophys. J. 589 (2003) L55.
[87] J. Knödlseder, M. Valsesia, M. Allain, et al., ESA SP 552 (2004) 33.
[88] N. Prantzos, Astron. Astrophys. 420 (2004) 1033.
[89] D. Smith, et al., ESA SP 552 (2004) 45.
[90] J. Knödlseder, E. Cisana, R. Diehl, et al., ESA SP 552 (2004) 123.
[91] W.N. Johnson, F.R. Harnden, R.C. Haymes, Astrophys. J. 172 (1972) L1.
[92] F. Albernhe, et al., Astron. Astrophys. 94 (1981) 214.
[93] M. Leventhal, C.J. MacCallum, P.D. Stang, Astrophys. J. 225 (1978) L11.
[94] M. Leventhal, Adv. Space Res. 11 (8) (1991) 157.
[95] G.R. Riegler, et al., Astrophys. J. 249 (1981) L13.
[96] G.H. Share, M.D. Leising, D.C. Messina, W.R. Purcell, Astrophys. J. 385 (1990) L45.
[97] W.A. Mahoney, J.C. Ling, W.A. Wheaton, Astrophys. J. Suppl. Ser. 92 (1993) 387.
[98] P. Milne, J. Kurfess, R.E. Kinzer, et al., AIP Conf. Proc. 587 (2001) 11.
[99] C.D. Dermer, J.G. Skibo, Astrophys. J. 487 (1997) L57.
[100] M.J. Harris, B.J. Teegarden, T.L. Cline, et al., Astrophys. J. 501 (1998) L55.
[101] W.A. Mahoney, J.C. Ling, W.A. Wheaton, R.E. Lingenfelter, Astrophys. J. Suppl. 92 (1994) 387.
[102] G.H. Share, R.L. Kinzer, J.D. Kurfess, et al., Astrophys. J. 326 (1988) 717.
[103] M. Leventhal, S.D. Barthelmy, N. Gehrels, et al., Astrophys. J. 405 (1993) L25.
[104] Ph. Durouchoux, et al., Astron. Astrophys. Suppl. Ser. 97 (1993) 185.
[105] P. Jean, P. von Ballmoos, J. Knödlseder, et al., ESA SP 552 (2004) 51.
[106] G. Weidenspointner, V. Lonjou, J. Knödlseder, et al., ESA SP 552 (2004) 133.
[107] E. Churazov, et al., astro-ph/0411351, Mon. Not. R. Astron. Soc., in press.
[108] J. Knödlseder, et al., Astron. Astrophys. (2005), in press.
[109] V. Lonjou, G. Weidenspointner, J. Knödlseder, et al., ESA SP 552 (2004) 129.
[110] A.W. Strong, R. Diehl, H. Halloin, et al., ESA SP 552 (2004) 507.
[111] N. Guessoum, P. Jean, J. Knödlseder, et al., ESA SP 552 (2004) 57.
[112] N. Guessoum, P. Jean, J. Gillard, Astron. Astrophys. (2005), in press.
[113] P. Jean, et al., Astron. Astrophys. (2005), in press.
[114] G. De Cesare, et al., Adv. Space Res. (2004), in press.
[115] K.-W. Chan, R. Lingenfelter, Astrophys. J. 405 (1993) 614.
[116] P.A. Milne, L.-S. The, M.D. Leising, Astrophys. J. Suppl. Ser. 124 (1999) 503.
[117] P.A. Milne, L.-S. The, M.D. Leising, Astrophys. J. 559 (2001) 503.
[118] K. Iwamoto, et al., Astrophys. J. Suppl. 125 (1999) 439.
[119] R. Launhardt, R. Zylka, P. Merger, Astron. Astrophys. 384 (2002) 112.
[120] L. Wang, P. Hoeffich, J.C. Wheeler, Astrophys. J. 483 (1997) L29.
[121] H.-J. Grimm, M. Gilfanov, R. Sunyaev, Astron. Astrophys. 39 (1) (2002) 923.
[122] C. Boehm, D. Hopper, J. Silk, et al., Phys. Rev. Lett. 92 (2004) 10;
      C. Boehm, D. Hopper, J. Silk, et al., Phys. Rev. Lett. 92 (2004) 1301.
[123] D. Hooper, et al., astro-ph/0311150.
[124] B. Cordier, et al., ESA SP 552 (2004) 581.
[125] A.W. Strong, I.V. Moskalenko, in: M. DuVernois (Ed.), Topics in Cosmic-Ray Astrophysics, Nova Scientific, New York, 1999.
[126] D.F. Torres, Phys. Rep. 382 (2003) 303.
[127] C.M.S. Cohen, et al., Geophys. Res. Lett. 26 (17) (1999) 2697.
[128] R.J. Murphy, et al., Astrophys. J. 490 (1997) 883.
[129] R.P. Lin, B.R. Dennis, G.J. Hurford, et al., Astrophys. J. 595 (2003) L69.
[130] H. Hudson, J. Ryan, Annu. Rev. Astron. Astrophys. 33 (1995) 239.
[131] R.W. Bussard, R. Ramaty, R.J. Drachman, Astrophys. J. 228 (1979) 928.
[132] G.H. Share, et al., Astrophys. J. 589 (2003) L85.

[133] G.H. Share, Astrophys. J. 589 (2003) L89.
[134] P. Mandrou, et al., ESA SP 382 (1997) 591.
[135] G.H. Share, et al., Astrophys. J. 508 (1998) 876.
[136] V. Tatischeff, et al., Phys. Rev. C 68 (2003) 5804.
[137] G.J. Hurford, et al., Astrophys. J. 595 (2003) L77.
[138] D. Smith, et al., Astrophys. J. 595 (2003) L81.
[139] M. Gros, V. Tatischeff, R. Diehl, et al., ESA SP 552 (2004) 669.
[140] R. Ramaty, et al., Astrophys. J. 316 (1979) 801.
[141] H. Bloemen, et al., Astron. Astrophys. 281 (1994) L5.
[142] H. Bloemen, et al., Astrophys. J. 521 (1999) L137.
[143] J.C. Higdon, Proc. ICRC 20 (1) (1987) 160.
[144] G. Vedrenne, J.-P. Roques, V. Schönfelder, et al., Astron. Astrophys. 411 (2003) L63.
[145] J.-P. Roques, S. Schanne, A. von Kienlin, et al., Astron. Astrophys. 411 (2003) L91.
[146] R.P. Lin, B.R. Dennis, G.J. Hurford, et al., Sol. Phys. 210 (2002) 3.
[147] A. Heger, et al., Astrophys. J. 591 (2003) 288.
[148] A.F. Iyudin, K. Bennett, H. Bloemen, et al., Astron. Astrophys. 300 (1995) 422.
[149] P. Jean, G. Vedrenne, J.-P. Roques, et al., Astron. Astrophys. 407 (2003) L55.
[150] P. Jean, J. Knödlseder, M. Hernanz, et al., ESA SP 552 (2004) 119.
[151] J. Jose, M. Hernanz, Astrophys. J. 494 (1998) 680.
[152] J. Knödlseder, V. Lonjou, P. Jean, et al., Astron. Astrophys. 411 (2003) L457.
[153] M. Limongi, A. Chieffi, Astrophys. J. 592 (2003) 404.
[154] R.J. Murphy, et al., Astrophys. J. 595 (2003) L93.
[155] U.G. Oberlack, et al., Astron. Astrophys. 353 (2000) 715.
[156] R. Ramaty, J. Skibo, R.E. Lingenfelter, Astrophys. J. Suppl. 92 (1994) 393.
[157] T. Tanaka, H. Washimi, Science 296 (2002) 321.
[158] E. Zinner, Annu. Rev. Earth Plan. Sci. 26 (1998) 147.
[159] M.J. Harris, et al., Astron. Astrophys. (2005), in press.
[160] R.L. Kinzer, et al., Astrophys. J. 559 (2001) 282.